JOURNAL OF CHEMICAL & ENGINEERING DATA

ARTICLE

pubs.acs.org/jced

Adsorption Equilibria of CO_2, CH_4, N_2, O_2, and Ar on High Silica Zeolites

Zongbi Bao,[†,‡] Liang Yu,[‡] Tao Dou,[§] Yanjun Gong,[§] Qing Zhang,[§] Qilong Ren,[†] Xiuyang Lu,[†] and Shuguang Deng[*,‡]

[†]Chemical and Biological Engineering Department, Zhejiang University, Hangzhou, 310027, China

[‡]Chemical Engineering Department, New Mexico State University, Las Cruces, New Mexico 88003, United States

[§]CNPC Key Laboratory of Catalysis, China University of Petroleum, Beijing, 102249, China

ABSTRACT: Adsorption equilibria of CO_2, CH_4, N_2, O_2, and Ar were determined on three lab-synthesized ZSM-5 adsorbents and four commercially available high silica zeolites including HiSiv-3000, HSZ-980HOA, HSZ-890HOA, and HSZ-390HUA. The synthesized ZSM-5 samples have a similar pore textural property (Brunauer−Emmett−Teller (BET) surface area and pore volume) as that of HiSiv-3000. The BET surface areas and total pore volume of the ZSM-5 sample were found to be ~300 $m^2 \cdot g^{-1}$ and 0.2 $cm^3 \cdot g^{-1}$, respectively. The synthesized materials have relatively higher adsorption capacities than those of HiSiv-3000 for the gases studied in this work. The order of adsorption capacities of CO_2, CH_4, N_2, Ar, and O_2 on each high silica zeolite follows the order of their polarizabilities. The selectivities of N_2/O_2 and Ar/O_2 pairs are close to 1.0, suggesting that it is very difficult to separate them by equilibrium-based adsorption processes. HSZ-890HOA and synthesized DT-100 showed higher equilibrium selectivities for CO_2 over N_2 and CH_4, implying that they are potential adsorbents for CO_2 separation from flue gases as well as landfill gases.

1. INTRODUCTION

The selective removal of carbon dioxide from gaseous mixtures is important for natural gas upgrading and carbon dioxide capture from flue gas. Carbon dioxide is a major impurity in various natural gases such as biogas, coal-seam, and landfill gases. These sources of natural gas primarily contain methane, carbon dioxide, and additional contaminants such as nitrogen, oxygen, water vapor, and sulfur compounds.[1] Flue gases released from coal-fired power plants typically contain around 17 % CO_2, 79 % N_2, and 4 % O_2 and trace contaminants such as water vapor.[2] Therefore, achievement in separation of carbon dioxide, methane, nitrogen, and oxygen mixtures cannot only upgrade low-quality natural gas but also mitigate the problem of excess CO_2 emission. Argon−oxygen separation is one of the difficult adsorption separation processes due to their similar physical properties.[3,4] Though high-purity oxygen and argon can be obtained by cryogenic distillation, the process might be highly energy-intensive. The adsorption-based separation process is considered as an energy- and cost-efficient alternative.

Through the emergence of various adsorbents and the development of adsorption-based separation processes, adsorption has become an important solution to the separation and purification of gases. Notable examples are N_2 production from air using carbon molecular sieves and separation of normal paraffins from isoparaffins and cyclic hydrocarbons on 5A zeolite.[5] For a practical adsorption process such as pressure swing adsorption (PSA) or vacuum swing adsorption (VSA), the selection of a proper adsorbent with adequate capacity and selectivity is critical to the overall economics of an adsorption process. Among all of the commercial adsorbents, synthetic zeolites (type A, 13X, and NaY) having low SiO_2/Al_2O_3 ratios have been widely used in commercial adsorption processes. However, carbon dioxide adsorption on these adsorbents is generally too strong, which will make regeneration difficult.[1,6] It is necessary to activate the material at a temperature over 300 °C to retain its high CO_2 adsorption capacity and selectivity. Moreover, some of the polar impurities in the feed gas such as water vapor and sulfur compounds could interact with these adsorbents much stronger than CO_2, resulting in a significant decrease of CO_2 capacity as well as a fluctuation in quality of product gas. Comparatively, high silica zeolites show a good compromise between high CO_2 selectivity and easy regeneration. As high silica zeolites have high SiO_2/Al_2O_3 ratios, only dispersion and polarization interactions are involved in the adsorption, and a high desorption rate can be easily achieved compared to hydrophilic adsorbents. More importantly, high silica zeolites can be used in the presence of water vapor and other polar contaminants.

ZSM-5 patented by Mobil Oil Company is a typical high silica hydrophobic zeolite, which has been widely used as a catalyst carrier for the isomerization reaction.[7−10] In this work, we have synthesized three ZSM-5 samples and investigated their adsorption properties for some of above-mentioned separations. For a further comparison we measured the adsorption properties of these gases on the other commercial high silica zeolites. These results will be useful for selecting adsorbents for gas separations in the presence of moisture.

2. EXPERIMENTAL SECTION

2.1. Materials. The silicalite sample HiSiv-3000 was purchased from UOP (USA). HiSiv-3000 has a same structure of ZSM-5 but with a larger SiO_2/Al_2O_3 ratio, which was reported as high as >1000.[6,11] The other high silica zeolites including H-ZSM-5 (HSZ-890HOA), Y zeolite (HSZ-390HUA), and β-zeolite (HSZ-980HOA) were kindly provided by Tosoh Co. (Japan).

Received: April 22, 2011
Accepted: September 21, 2011
Published: October 07, 2011

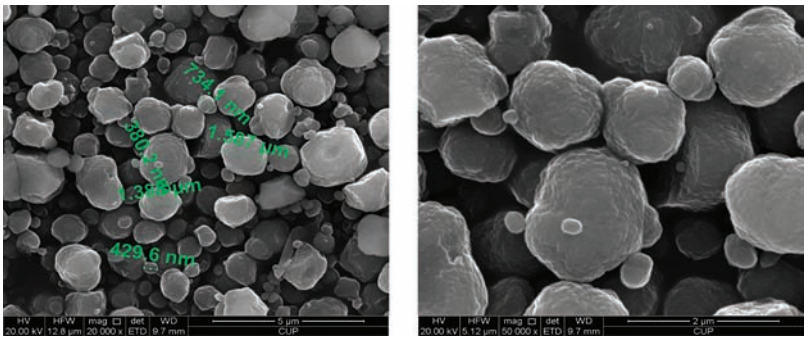

Figure 1. Scanning electron micrographs of synthesized DT-100 powder.

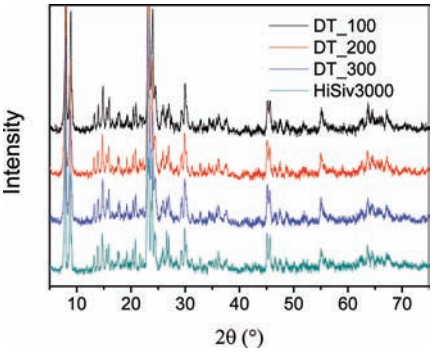

Figure 2. XRD patterns of synthesized ZSM-5 samples and UOP HiSiv3000.

Silica-sol (SiO_2, 40 wt %, Qingdao Haiyang Chemical Co.) was used as the silica source for synthesis of ZSM-5 adsorbents in this work. Sodium aluminate ($NaAlO_2$, AR (analytical reagent)) and sodium hydroxide (NaOH, AR) were purchased from Sinopharm Chemical Reagent Co., Ltd. Tetrapropylammonium hydroxide (TPAOH, 35 %) and tetrapropylammonium bromide (TPABr, 99 %) were purchased from Xi'nan Chemical Institute. Besides, reagent-grade glycerin ($C_3H_8O_3$), OP-10 ($C_{34}H_{62}O_{11}$), and citric acid ($C_6H_8O_7$) were also used, and all of them were purchased from Tianjin Kermel Chemical Reagent Co., Ltd.

2.2. Synthesis of ZSM-5. First, we prepared a structure-directing agent that is important for forming the desired pores of ZSM-5. The structure-directing agent was prepared as follows. Microemulsions were obtained after dissolving 11.2 g of emulsifier (OP-10) in 9.8 mL of deionized water at 30 °C, to which 56.2 g of tetrapropylammonium hydroxide (TPAOH) was added and followed by 76.2 g of silica-sol. The resulted mixture was further stirred strongly for 2 h until it was homogenously dispersed and then transferred to a Teflon-lined stainless steel autoclave. The autoclave was capped tightly and placed in an oven at 120 °C for 12 h. After the reaction was completed, the product was cooled down to room temperature and used in the following steps.

Second, ZSM-5 zeolite was synthesized as follows: 1.68 g of sodium aluminate ($NaAlO_2$) and 206.56 g of silica-sol were added to a solution of 11.45 g of sodium hydroxide (NaOH) in 80 mL of deionized water successively and then stirred vigorously for 1 h to form mixture A. Mixture B was prepared by adding 13.6 g of above structure-directing agent into a solution of 26.4 g of tetrapropylammonium bromide (TPABr) in 80 mL of deionized water and 36 mL of glycerin under a strong agitation. After 30 min, mixture B was added slowly to mixture A under stirring. Then, the final reactant was further mixed under sonication and then

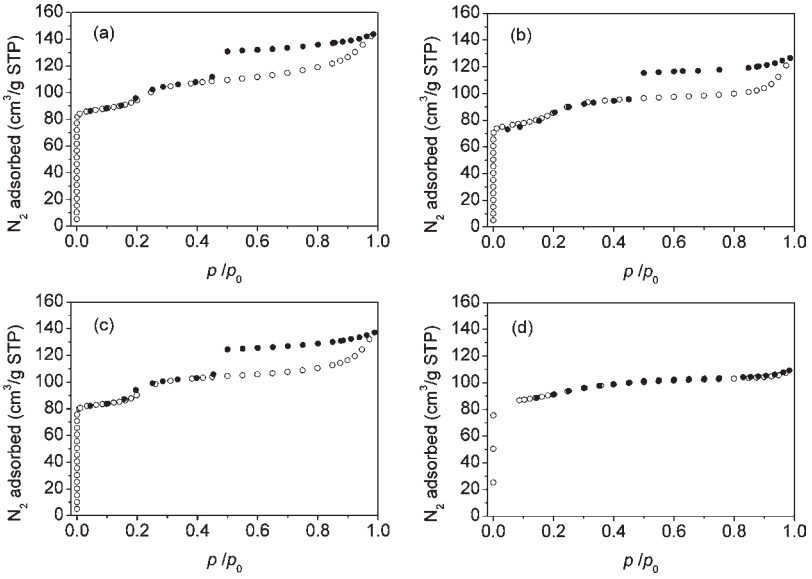

Figure 3. N_2 adsorption isotherms of synthesized samples and UOP adsorbent at 77 K: (a) DT-100; (b) DT-200; (c) DT-300; (d) HiSiv 3000.

Table 1. Physical Properties of Adsorbents Tested in This Study

property	980HOA	890HOA	390HUA	DT-100	DT-200	DT-300	HiSiv-3000
BET surface area ($m^2 \cdot g^{-1}$)	480 ± 13.3	351 ± 10.4	728 ± 22.8	311 ± 3.9	292 ± 0.8	302 ± 3.8	295 ± 1.2
pore volume ($cm^3 \cdot g^{-1}$)	0.311	0.203	0.572	0.222	0.196	0.212	0.169
median pore width (Å)	6.8	5.1	9.3	6.0	6.0	6.0	5.9
SiO_2/Al_2O_3	480	2120	750	117	185	152	46

transferred to a stainless steel autoclave. After the reactants were aged for 24 h at a room temperature, the autoclave was capped tightly and heated up to 170 °C. Crystallization took place under autogenous pressure for 48 h, and then the autoclave was quenched. The filtered product was washed and dried at 110 °C overnight.

Finally, the extrudate of ZSM-5 was made from the mixture containing as-synthesized ZSM-5 powder and silica-sol (20 wt % in SiO_2) using a twin-screw extruder. The shaped adsorbents were dried at 110 °C and calcined at 500 °C for 6 h to remove templates and extrusion assistant. The obtained adsorbent was labeled as DT-100.

To increase the SiO_2/Al_2O_3 ratio, DT-100 was further treated by 1 $mol \cdot L^{-1}$ nitric acid or 1 $mol \cdot L^{-1}$ citric acid to remove partial aluminum atoms. The adsorbents were treated under a reflux at 70 °C for 2 h and then washed with water to remove the residual acid. The resulted adsorbents were obtained after drying and activation under an air atmosphere at 500 °C for 4 h. The adsorbents treated by nitric acid and citric acid were labeled as DT-200 and DT-300, respectively.

2.3. Characterization of Adsorbents. The particle morphologies of the synthesized ZSM-5 samples and commercial adsorbent were observed by a Hitachi TM-1000 scanning electron microscope (SEM) at an accelerating voltage of 15 kV. Elemental analysis of the synthesized samples was performed using an energy dispersive spectrometer (EDS). Its crystallinity was confirmed by powder X-ray diffraction (PXRD). The XRD patterns were recorded using a Rigaku Miniflex-II X-ray diffractometer with Cu Kα (λ = 1.5406 Å) radiation, 30 kV/15 mA current, and kβ-filter. A step scan with an increment of 0.02° in 2θ and a scan rate of 0.2 $deg \cdot min^{-1}$ was applied to obtain the high-resolution patterns. A Micromeritics ASAP 2020 adsorption porosimeter was used to measure the N_2 adsorption isotherms at 77 K. The pore textural properties including Brunauer–Emmett–Teller (BET) surface area, pore volume, and pore size distribution were obtained from the N_2 adsorption and desorption isotherms.

2.4. Adsorption Isotherm Measurements. Equilibrium adsorption isotherms of CO_2, CH_4, N_2, O_2, and Ar in all adsorbents were measured volumetrically in a Micromeritics ASAP 2020 adsorption apparatus. The adsorption isotherms were measured at 298 K and gas pressure up to 1 atm using the same procedure. All samples used in this work were degassed at 623 K under dynamic vacuum (10^{-5} mmHg) overnight. The weight of sample was determined before and after activation. The free space of the system was determined by using the helium gas. Ultrahigh purity grade CO_2, CH_4, N_2, O_2, Ar, and He from Matheson Co. were used as received.

For convex isotherms the adsorption equilibrium data were fitted by the Langmuir equation,

$$q = q_m \frac{bP}{1 + bP} \quad (1)$$

where q ($mmol \cdot g^{-1}$) is the adsorbed amount; p (kPa) is the equilibrium pressure; q_m ($mmol \cdot g^{-1}$) is the monolayer adsorption capacity; and b (kPa^{-1}) is the Langmuir adsorption equilibrium constant. Henry's law constant can be calculated as $K = q_m b$.

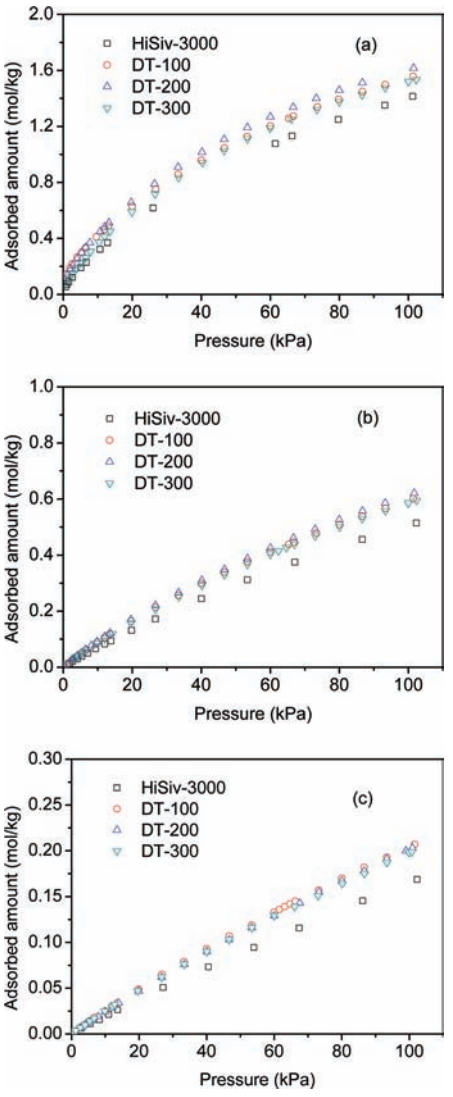

Figure 4. Adsorption of CO_2 (a), CH_4 (b), and N_2 (c) on UOP HiSiv-3000 and synthesized samples at 298 K.

Using the Langmuir model equation to fit the equilibrium data for quite linear isotherms will gender a great uncertainty on model parameters. In this case, Henry's law was used to correlate the equilibrium data:

$$q = Kp \quad (2)$$

The ratio of Henry's constants of gas A over B was used to calculate the intrinsic selectivity:

$$\alpha_{A/B} = K_A/K_B \quad (3)$$

dx.doi.org/10.1021/je200394p |J. Chem. Eng. Data 2011, 56, 4017–4023

Table 2. Model Parameters of the Langmuir Isotherm or Henry's Law Constants for Pure Gas Adsorption at 298 K

adsorbate	DT-100		HSZ-980HOA		HSZ-890HOA		HSZ-390HUA	
CO_2	q_m	2.19 ± 0.11	q_m	3.91 ± 0.05	q_m	3.64 ± 0.01		
	b (10^{-3})	1	b (10^{-3})	5	b (10^{-3})	1		
	K (10^{-3})	21.3 ± 2.3	K (10^{-3})	6.89 ± 0.1	K (10^{-3})	12.9 ± 0.0	K (10^{-3})	6.22 ± 0.1
	ARE[a] (%)	2	ARE (%)	4	ARE (%)	3	ARE (%)	1
		46.6 ± 2.9		26.9 ± 0.1		46.9 ± 0.5		2.2
		4		8		4		
		13.4		5.3		0.53		
CH_4	q_m	1.68 ± 0.03	q_m	2.14 ± 0.07	q_m	2.97 ± 0.02	q_m	4.87 ± 0.39
	b (10^{-3})	3	b (10^{-3})	7	b (10^{-3})	2	b (10^{-3})	9
	K (10^{-3})	5.43 ± 0.1	K (10^{-3})	2.22 ± 0.0	K (10^{-3})	2.99 ± 0.0	K (10^{-3})	0.407 ± 0
	ARE (%)	1	ARE (%)	8	ARE (%)	2	ARE (%)	0.3
		9.12 ± 0.0		4075 ± 0.0		8.88 ± 0.0		1.98 ± 0.0
		5		3		1		1
		2.5		2.6		0.81		1.1
N_2	q_m	0.998 ± 0.0	q_m	0.848 ± 0.0				
	b (10^{-3})	0.2	b (10^{-3})	0.9				
	K (10^{-3})	2.57 ± 0.06	K (10^{-3})	1.95 ± 0.03	K (10^{-3})	2.04 ± 0.00	K (10^{-3})	0.879 ± 0.0
	ARE (%)	6	ARE (%)	3	ARE (%)	0.4	ARE (%)	0.02
		2.56 ± 0.0		1.65 ± 0.0		2.3		2.6
		0.68		3.8				
O_2	K (10^{-3})	1.77 ± 0.01	K (10^{-3})	1.46 ± 0.01	K (10^{-3})	2.14 ± 0.01	K (10^{-3})	0.898 ± 0.0
	ARE (%)	1	ARE (%)	1	ARE (%)	1	ARE (%)	0.03
		5.0		9.3		4.1		7.9
Ar	K (10^{-3})	1.78 ± 0.01	K (10^{-3})	1.43 ± 0.01	K (10^{-3})	2.42 ± 0.01	K (10^{-3})	0.984 ± 0.0
	ARE (%)	1	ARE (%)	1	ARE (%)	1	ARE (%)	0.02
		4.2		4.8		2.1		1.4

[a] $$\mathrm{ARE} = \frac{100}{N} \cdot \sum_{k=1}^{N} \left| \frac{q_{exp} - q_{cal}}{q_{exp}} \right|_k .$$

Table 3. Comparison of Adsorption Capacities with Literature Data

literature[14−17]				this work			
adsorbate	adsorbent	conditions	capacities (mmol·g^{-1})	adsorbate	adsorbent	conditions	capacities (mmol·g^{-1})
CO_2	silicalite	30.6 °C, 600 Torr	1.4	CO_2	HSZ-890	25.0 °C, 760 Torr	2.068
CO_2	NaZSM-5	24.1 °C, 540 Torr	1.9	CO_2	DT-100	25.0 °C, 760 Torr	1.557
CH_4	silicalite	23.07 °C, 700 Torr	0.7	CH_4	HSZ-890	25.0 °C, 760 Torr	0.692
CH_4	NaZSM-5	23.3 °C, 600 Torr	0.75	CH_4	DT-100	25.0 °C, 760 Torr	0.601
N_2	silicalite	22.95 °C, 700 Torr	0.2	N_2	HSZ-890	25.0 °C, 760 Torr	0.206
N_2	NaZSM-5	21.9 °C, 760 Torr	0.3	N_2	DT-100	25.0 °C, 760 Torr	0.207
O_2	silicalite	32.30 °C, 760 Torr	0.15	O_2	HSZ-890	25.0 °C, 760 Torr	0.214
				O_2	DT-100	25.0 °C, 760 Torr	0.176
Ar	silicalite	32.60 °C, 700 Torr	0.14	Ar	HSZ-890	25.0 °C, 760 Torr	0.240
Ar	NaZSM-5	23.2 °C, 800 Torr	0.25	Ar	DT-100	25.0 °C, 760 Torr	0.177

3. RESULTS AND DISCUSSION

3.1. Characterization of Adsorbents. Figure 1 shows the SEM images of a synthesized ZSM-5 in this work. It can be seen that its morphology is intergrown aggregates of plate-like crystals as observed in other high silica zeolites.[12,13] The particle size of obtained sample ranges from (0.4 to 2) μm. The elemental analysis of the sample using EDS shows that the SiO_2/Al_2O_3 ratio is 117, which is much higher than that of HiSiv-3000. The ratio of SiO_2/Al_2O_3 for HiSiv-3000 is 46 when determined at the same condition, but it is far less than the reported value (>1000). The XRD patterns of synthesized ZSM-5 samples along with that of HiSiv-3000 are given in Figure 2. Since adsorbent HisSiv-3000 is based on the ZSM-5 structure, the XRD patterns of these samples show almost identical phase characteristics. N_2 adsorption isotherms at 77 K of synthesized sample and HiSiv-3000 are

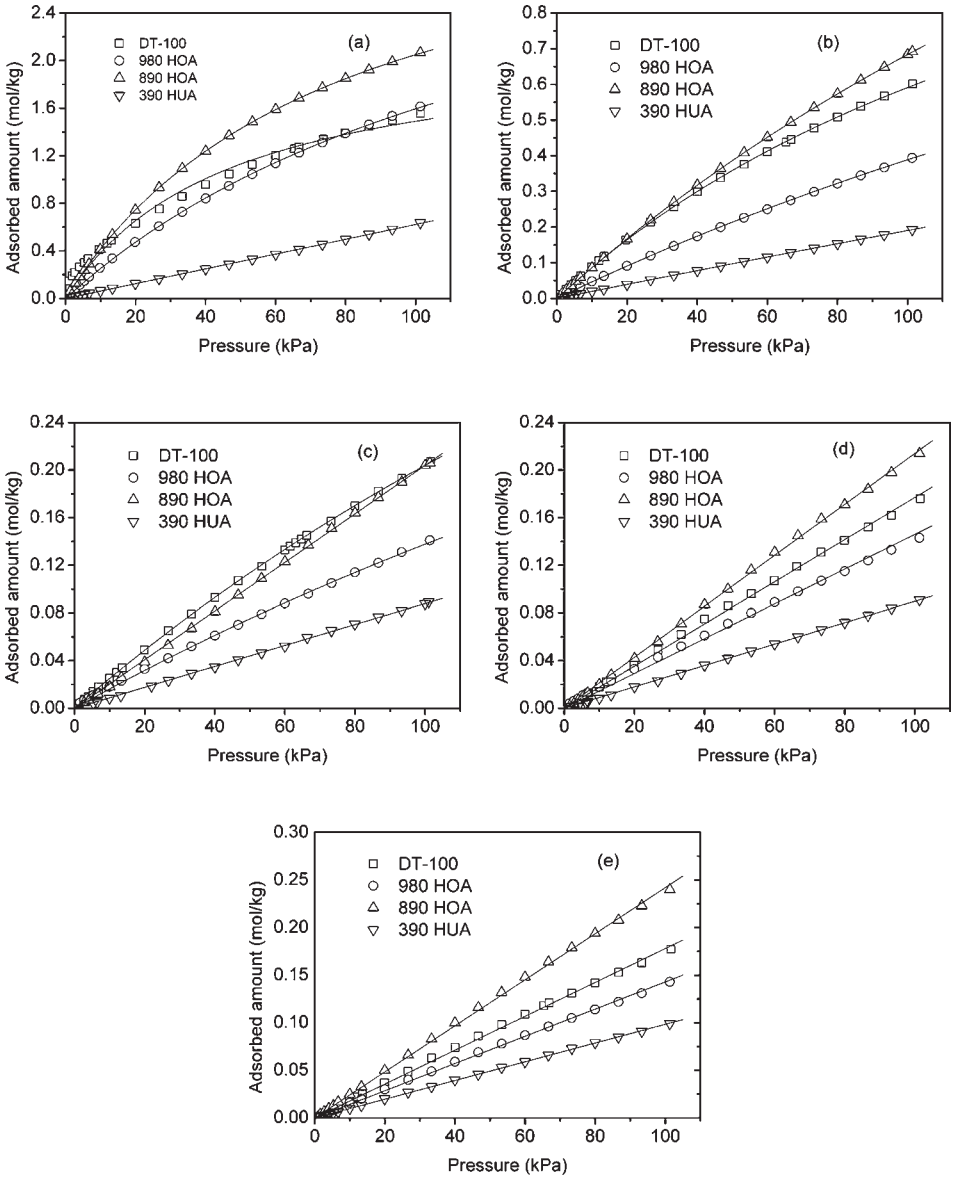

Figure 5. Equilibrium adsorption isotherms of (a) CO_2, (b) CH_4, (c) N_2, (d) O_2, and (e) Ar on DT-100, HSZ-980HOA, HSZ-890HOA, and HSZ-390HUA at 298 K.

shown in Figure 3, and the properties including BET surface area, pore volume, and average pore size calculated from these isotherms are summarized in Table 1. As seen from the Figure 3, the adsorption isotherms of N_2 at 77 K of the synthesized samples are quite different from that of the UOP samples. Adsorption−desorption hysteresis loops corresponding to mesopores can be clearly observed on the synthesized samples. However, the adsorption uptake of all of the samples at a low-pressure region increases very sharply, indicating that these adsorbents are typical microporous materials. Their media pore width calculated by the Horvath−Kwazoe (H−K) method fell at ~6 Å, which is in agreement with the previously reported value.[6,12] The BET surface areas and total pore volume were found to be about 300 $m^2 \cdot g^{-1}$ and 0.2 $cm^3 \cdot g^{-1}$, respectively. Compared to HiSiv-3000, the BET surface areas of our samples except DT-200 are slightly larger, and the pore volumes are much higher because of a lower aluminum content in the zeolite framework so that less Na^+ cations are required to balance the charge in the channel.

Table 4. Equilibrium Adsorption Selectivities of Gases on Different Adsorbents at 298 K

	adsorption selectivity				
adsorbent	CO_2/CH_4	CO_2/N_2	CH_4/O_2	N_2/O_2	Ar/O_2
DT-100	5.1	18.2	5.2	1.4	1.0
HSZ-980HOA	5.7	16.3	2.9	1.1	0.98
HSZ-890HOA	5.3	23.0	4.1	0.95	1.1
HSZ-390HUA	3.1	7.1	2.2	0.98	1.1

To compare the uptake capacity between the synthesized and the commercial adsorbents, we performed pure CO_2, CH_4, and N_2 adsorption on these samples. The adsorption

dx.doi.org/10.1021/je200394p |J. Chem. Eng. Data 2011, 56, 4017–4023

equilibrium data were displayed in Figure 4. It shows that the synthesized materials have similar but relatively higher adsorption capacities than those of the commercial zeolite samples for all gases. A minor difference in the adsorption amount on the synthesized samples suggests that surface properties of the zeolite materials did not change significantly after the acid treatment.

3.2. Pure Gas Adsorption Isotherms. The single-component adsorption isotherms of CO_2, CH_4, N_2, O_2, and Ar on DT-100, HSZ-890HOA, HSZ-390HUA, and HSZ-980HOA at 298 K are plotted in Figure 5. The adsorption isotherms of CO_2 and CH_4 are of type-I isotherm, while the isotherms of N_2, O_2, and Ar are more or less linear. The solid lines in the figure represent the best regressed form of the Langmuir isotherm equation or Henry's law. Table 2 summarizes the isotherm model parameters along with their corresponding absolute relative error (ARE) values. From the plots in Figure 5 it can be observed that the adsorption capacities of the gases studied in this work at a pressure of 1 atm decreased in the following order:

HSZ-890 > DT-100 > HSZ-980 > HSZ-390

The adsorption capacities on HSZ-890 were found to be (2.068, 0.692, 0.206, 0.214, and 0.240) mol·kg^{-1} for CO_2, CH_4, N_2, O_2, and Ar, respectively, at 1 atm and 298 K. In the case of DT-100, the adsorption capacities of corresponding gases were (1.557, 0.601, 0.207, 0.176, and 0.177) mol·kg^{-1}. As shown in Table 3, these adsorption capacities were comparable to the reported values on ZSM-5 or silicalite samples.[14−17] It should be pointed that it is difficult to find literature data on the ZSM-5 type of zeolites of the same SiO_2/Al_2O_3 ratios at identical experimental conditions investigated in this work.

Among all of the studied gases, CO_2 and CH_4 were preferably adsorbed on studied adsorbents compared to N_2, O_2, and Ar. High silica zeolites, that is, DT-100 and HSZ-890, have comparable values for the Henry's constants for CO_2 and CH_4. Since only the dispersion and polarization interactions are involved in the adsorption by high silica zeolites, it can be found that their adsorption capacities follows the order, $CO_2 > CH_4 > N_2 > Ar \approx O_2$, which is consistent with the order of their polarizability with the corresponding value of 29.1, 25.9, 17.4, 16.4, and 15.8 ($\cdot 10^{-25}$ cm^3), respectively.[18] Due to the similar polarizability between oxygen and nitrogen or argon, the equilibrium selectivities on all adsorbents are very close to unity. It seems impossible to separate Ar/O_2 or N_2/O_2 mixtures by an equilibrium-based adsorption process. Such observations on ZSM-5 of different ratios were also reported by Sethia et al.[19]

Table 4 shows the equilibrium adsorption selectivities of gases on different adsorbents, which were calculated from the ratio of their Henry's law constants in Table 2. From the table, it can be seen that the highest selectivity of CO_2 over N_2 was obtained on these adsorbents. The selectivities of CO_2 over N_2 on DT-100 and HSZ-890 are as high as 18.2 and 23, respectively, suggesting they are potential adsorbents for CO_2 separation from flue gas, which contains N_2 and CO_2 in substantive amounts. High silica zeolites also show higher equilibrium selectivity for CO_2 over CH_4; the equilibrium selectivities reach up to 5.1 and 5.3, respectively. Therefore, it can also be used as a potential adsorbent for the separation of methane from landfill gas. However, HSZ-390HUA shows moderate selectivities even for CO_2/CH_4 and CO_2/N_2 separation. Even though HSZ-980 has similar selectivities for these gas components, comparatively, it has lower adsorption capacities. Therefore, this suggests that the synthesized ZSM-5 adsorbent and HSZ-890 are more suitable for the adsorption separation of gas mixtures containing CO_2, CH_4, and N_2. However, if moisture is not a concern, adsorbents (zeolite NaX, zeolite 5A, Mg-MOF-74, MOF-5, MOF-177, and Cu-MOF) with a much higher equilibrium selectivity[20,21] or kinetic selectivity[22] for CO_2/CH_4 and CO_2/N_2 separation are available.

4. CONCLUSIONS

Three ZSM-5 adsorbent samples were synthesized and characterized with SEM and BET. One synthesized ZSM-5 adsorbent (DT-100) and a few high silica zeolites from Tosh. Co. were evaluated for their adsorption of CO_2, CH_4, N_2, O_2, and Ar. The synthesized ZSM-5 adsorbents have a similar pore textural property as that of HiSiv-3000 and relatively higher adsorption capacities of CO_2, CH_4, and N_2 than those of HiSiv-3000. The adsorption capacities of these gases on two selected high silica zeolites (HSZ-890HOA and DT-100) are comparable to the reported adsorption capacities on ZSM-5 and silicalite adsorbents. The adsorption capacities of these gases follow the order of their polarizabilities. The selectivities of N_2/O_2 and Ar/O_2 pairs being close to 1.0 suggest that it is difficult to separate them by an equilibrium-based adsorption process. The high silica zeolites studied in this work, that is, HSZ-890HOA and DT-100, showed higher equilibrium selectivities for CO_2/N_2 and CO_2/CH_4 separation, suggesting they are potential adsorbents for CO_2 separation from flue gases as well as landfill gas.

AUTHOR INFORMATION

Corresponding Author
*E-mail: sdeng@nmsu.edu.

REFERENCES

(1) Delgado, J. A.; Uguina, M. A.; Sotelo, J. L.; Ruiz, B.; Gomez, J. M. Fixed-bed adsorption of carbon dioxide/methane mixtures on silicalite pellets. *Adsorption* **2006**, *12*, 5–18.

(2) Kikkinides, E. S.; Yang, R. T.; Cho, S. H. Concentration and recovery of CO_2 from flue gas by pressure swing adsorption. *Ind. Eng. Chem. Res.* **1993**, *32*, 2714–2720.

(3) Jin, X.; Malek, A.; Farooq, S. Production of argon from an oxygen-argon mixture by pressure swing adsorption. *Ind. Eng. Chem. Res.* **2006**, *45*, 5775–5787.

(4) Rege, S. U.; Yang, R. T. Kinetic separation of oxygen and argon using molecular sieve carbon. *Adsorption* **2000**, *6*, 15–22.

(5) Sircar, S. Basic research needs for design of adsorptive gas separation processes. *Ind. Eng. Chem. Res.* **2006**, *45*, 5435–5448.

(6) Harlick, P. J. E.; Tezel, F. H. An experimental adsorbent screening study for CO_2 removal from N_2. *Microporous Mesoporous Mater.* **2004**, *76*, 71–79.

(7) Seo, G.; Jeong, H. S.; Hong, S. B.; Uh, Y. S. Skeletal isomerization of 1-butene over ferrierite and ZSM-5 zeolites: Influence of zeolite acidity. *Catal. Lett.* **1996**, *36*, 249–253.

(8) Werst, D. W.; Tartakovsky, E. E.; Piocos, E. A.; Trifunac, A. D. Isomerization of olefin radical cations in ZSM-5 zeolites. *J. Phys. Chem.* **1994**, *98*, 10249–10257.

(9) Tarditi, A. M.; Horowitz, G. I.; Lombardo, E. A. Xylene isomerization in a ZSM-5/SS membrane reactor. *Catal. Lett.* **2008**, *123*, 7–15.

(10) Villegas, J. I.; Kumar, N.; Heikkila, T.; Lehto, V. P.; Salmi, T.; Murzin, D. Y. Isomerization of n-butane to isobutane over Pt-modified Beta and ZSM-5 zeolite catalysts: Catalyst deactivation and regeneration. *Chem. Eng. J.* **2006**, *120*, 83–89.

(11) Choi, S.; Drese, J. H.; Jones, C. W. Adsorbent materials for carbon dioxide capture from large anthropogenic point sources. *ChemSusChem* **2009**, *2*, 796–854.

(12) Pillai, R. S.; Peter, S. A.; Jasra, R. V. Adsorption of carbon dioxide, methane, nitrogen, oxygen and argon in NaETS-4. *Microporous Mesoporous Mater.* **2008**, *113*, 268–276.

(13) Kim, W. J.; Lee, M. C.; Hayhurst, D. T. Synthesis of ZSM-5 at low temperature and atmospheric pressure in a pilot-scale batch reactor. *Microporous Mesoporous Mater.* **1998**, *26*, 133–141.

(14) Golden, T. C.; Sircar, S. Gas adsorption on silicalite. *J. Colloid Interface Sci.* **1994**, *162*, 182–188.

(15) Dunne, J. A.; Mariwals, R.; Rao, M.; Sircar, S.; Gorte, R. J.; Myers, A. L. Calorimetric heats of adsorption and adsorption isotherms. 1. O_2, N_2, Ar, CO_2, CH_4, C_2H_6 and SF_6 on silicalite. *Langmuir* **1996**, *12*, 5888–5895.

(16) Dunne, J. A.; Rao, M.; Sircar, S.; Gorte, R. J.; Myers, A. L. Calorimetric heats of adsorption and adsorption isotherms. 2. O_2, N_2, Ar, CO_2, CH_4, C_2H_6, and SF_6 on NaX, H-ZSM-5, and Na-ZSM-5 zeolites. *Langmuir* **1996**, *12*, 5896–5904.

(17) Harlick, P. J. E.; Tezel, F. H. Adsorption of carbon dioxide, methane, and nitrogen: Pure and binary mixture adsorption by ZSM-5 with SiO_2/Al_2O_3 ratio of 30. *Sep. Sci. Technol.* **2002**, *37*, 33–60.

(18) Li, J. R.; Kuppler, R. J.; Zhou, H. C. Selective gas adsorption and separation in metal-organic frameworks. *Chem. Soc. Rev.* **2009**, *38*, 1477–1504.

(19) Sethia, G.; Pillai, R. S.; Dangi, G. P.; Somani, R. S.; Bajaj, H. C.; Jasra, R. V. Sorption of methane, nitrogen, oxygen, and argon in ZSM-5 with different SiO_2/Al_2O_3 ratios: Grand canonical monte carlo simulation and volumetric measurements. *Ind. Eng. Chem. Res.* **2010**, *49*, 2353–2362.

(20) Bao, Z.; Yu, L.; Ren, Q.; Lu, X.; Deng, S. Adsorption of CO_2 and CH_4 on a magnesium-based metal-organic framework. *J. Colloid Interface Sci.* **2011**, *353*, 549–556.

(21) Saha, D.; Bao, Z.; Feng, J.; Deng, S. Adsorption of CO_2, CH_4, N_2O and N_2 on MOF-5, MOF-177 and Zeolite 5A. *Environ. Sci. Technol.* **2010**, *44*, 1820–1826.

(22) Bao, Z.; Alnemrat, S.; Yu, L.; Vasiliev, I.; Ren, Q.; Lu, X.; Deng, S. Kinetic Separation of CO_2/CH_4 in Microporous Metal-Organic Frameworks. *J. Colloid Interface Sci.* **2011**, *357*, 504–509.